Published in final edited form as:
Gut. 2014 April ; 63(4): 540–551. doi:10.1136/gutjnl-2013-304612.

Glutathione peroxidase 7 has potential tumor suppressor functions that are silenced by location-specific methylation in oesophageal adenocarcinoma

DunFa Peng[1,2], **TianLing Hu**[1,2], **Mohammed Soutto**[1,2], **Abbes Belkhiri**[2], **Alexander Zaika**[2], and **Wael El-Rifai**[1,2]

[1]Department of Veterans Affairs, Tennessee Valley Healthcare System, Nashville, TN 37232

[2]Department of Surgery, Vanderbilt University Medical Center, Nashville TN 37232

Abstract

Objective—We investigated the potential tumor suppressor functions of glutathione peroxidase 7 (GPX7) and examined the interplay between epigenetic and genetic events in regulating its expression in oesophageal adenocarcinomas (OAC).

Design—In vitro and in vivo cell models were developed to investigate the biological and molecular functions of GPX7 in OAC.

RESULTS—Reconstitution of GPX7 in OAC cell lines, OE33 and FLO-1, led to significant growth suppression as demonstrated by growth curve, colony formation and EdU proliferation assays. Meanwhile, GPX7-expressing cells displayed significant impairment in G1/S progression and an increase in cell senescence. Concordant with the above functions, Western blot analysis displayed higher levels of p73, p27, p21, and p16 with a decrease in phosphorylated RB; indicating its increased tumor suppressor activities. On the contrary, knockdown of GPX7 in HET1A cells (an immortalized normal esophageal cell line) rendered the cells growth advantage as indicated with a higher EdU rate, lower levels of p73, p27, p21, and p16 and an increase in phosphorylated RB. We confirmed the tumor suppressor function in vivo using GPX7-expressing OE33 cells in a mouse xenograft model. Pyrosequencing of the GPX7 promoter region (−162 to +138) demonstrated location-specific hypermethylation between +13 and +64 in OACs (69%, 54/78). This was significantly associated with the downregulation of GPX7 ($p<0.01$). Neither mutations in the coding exons of GPX7 nor DNA copy number losses were present in the OACs examined (<5%).

CONCLUSIONS—Our data suggest that GPX7 possesses tumor suppressor functions in OAC and is silenced by location-specific promoter DNA methylation.

[*]**Corresponding Author:** Wael El-Rifai, Vanderbilt-Ingram Cancer Center, Vanderbilt University Medical Center, 1255 Light Hall, 2215 Garland Avenue, Nashville, TN 37232. wael.el-rifai@vanderbilt.edu.

Contributorship:
DP: biological assays, methylation analysis, and manuscript writing
TH: PCR experiments
MS: assisted in animal studies
AB: experimental design, troubleshooting, reviewed the written draft
AZ: troubleshooting, interpretation of results
WER: study design, interpretation of results, troubleshooting, manuscript writing

Competing interests: All the authors declared no conflict of interest for the purpose of this study.

Keywords

GPX7; Barrett's; cancer; tumor suppressor; DNA methylation

Introduction

The incidence rate for OAC has increased 4–10% per year among men since 1976, more rapidly than for any other type of cancers [1]. Barrett's oesophagus (BO), a pre-cancerous condition in which the original oesophageal squamous epithelia are replaced by columnar epithelia due to chronic gastro-oesophageal reflux disease (GORD), is the main risk factor for development of OAC [2–4]. Patients with Barrett's oesophagus can progress to low-grade dysplasia, high-grade dysplasia and OAC at 30–60 times that of the general population [4–6]. The natural and molecular history of the progression of Barrett's oesophagus to OAC remains poorly characterized.

Glutathione peroxidase (GPX) is a major antioxidant enzyme family that catalyses the reduction of hydrogen peroxide (H_2O_2), organic hydroperoxide, and lipid peroxides by reduced glutathione [7, 8]. There are eight members of GPX, GPX1-GPX8. GPX7 was first identified from cDNAs amplified from mRNA of *Brca1*-null mouse embryonic fibroblasts [9]. Recently, GPX7 was identified to have limited glutathione peroxidase activity, although it can neutralize H_2O_2 in vitro without the existence of glutathione [10]. Expression of GPX7 can protect normal oesophageal epithelia from acidic bile salts-induced oxidative stress, oxidative DNA damage and double strand breaks [10]. Frequent dysfunction of GPX7 in OAC and its precancerous Barrett's dysplasia [11] suggest that impairment of the antioxidant capacity may contribute to the development of OAC. However, the full spectrum of the molecular functions of GPX7 has not been established. In the present study, we examined the possible tumor suppressor function of GPX7 in vitro and in vivo and determined the possible epigenetic and genetic mechanisms that could regulate its expression in OAC.

Materials and Methods

Cell lines

Three immortalized cell lines originated from normal oesophageal squamous epithelia: HEEC (ScienCell Research Laboratories, Carlsbad, California, USA), EPC2 (kindly provided by Dr. Hiroshi Nakagawa), and HET1A (purchased from American Type Culture Collection (ATCC), Manassas, Virginia, USA). Four immortalized cell lines originated from Barrett's oesophagus: BAR-T, BAR-T10 (kindly provided by Dr. Rhonda Souza), CP-A, and CP-B (purchased from ATCC). Lastly, five oesophageal adenocarcinoma cell lines were used in this study: OE19 (purchased from Sigma-Aldrich, St. Louis, Missouri, USA), OE33, FLO-1, SKGT4, and JH-Eso-Ad1 (a gift from Drs. David Beer and Jim Eshleman). FLO-1, OE33 and HET1A were used in the functional experiments while other cell lines were used in gene expression, DNA methylation, DNA copy number, and mutation analysis. The HEK293 AD cell line (Cell Biolabs Inc, San Diego, California, USA) was used for propagating adenoviral particles. All cell lines were grown at 37°C in 5% carbon dioxide following the recommended procedures.

Tissue samples

All de-identified tissue samples were obtained from the archives of pathology at Vanderbilt University (Nashville, Tennessee, USA) and from the National Cancer Institute Cooperative Human Tissue Network (CHTN). The use of specimens from the tissue repository was

approved by the Vanderbilt Institutional Review Board. For DNA and mRNA analysis, 148 frozen tissue samples (78 OACs, 6 Barrett's oesophagus, 36 normal oesophagus, and 28 normal stomach samples) were collected. All adenocarcinomas were classified according to the recent guidelines of the International Union Against Cancer (UICC) TNM classification system. All OAC originated from the lower oesophagus or gastro-oesophageal junction corresponding to AEG Type 1 as previously described [12]. The patients' ages ranged from 34–82 years (median at 63 years). The adenocarcinomas ranged from well differentiated to poorly differentiated, stages I–IV, with a mix of intestinal- and diffuse-type tumors.

Cloning and construction of GPX7 expression plasmids

A full length of GPX7 coding sequence with Flag-tag was amplified from normal cDNA by PCR and was cloned into the pcDNA 3.1 and pACCMV.pLpA plasmids [10]. The GPX7 expressing adenoviral system was then constructed as previously described [13]. Two oesophageal adenocarcinoma cell lines (FLO-1 and OE33) in which GPX7 expression was significantly downregulated, were transfected with control or GPX7-pcDNA plasmids using Lipofectamine 2000 transfection reagent (Life Technologies, Grand Island, New York, USA), or were infected with 25 multiplicity of infection (MOI) per cell of adenoviral GPX7 particles (Ad-GPX7) and adenoviral empty particles (Ad-CTRL) in the culture medium. Forty-eight hours after infection, the cells were harvested and validated for the expression of GPX7 using quantitative RT-PCR and Western blotting.

Knockdown of GPX7 expression by lentiviral shRNA

To knockdown GPX7 expression in non-malignant cells, the oesophageal squamous cell line HET1A was transfected with the same MOI of scrambled short hairpin RNA controls (Sc shRNA) and GPX7 validated specific shRNA (GPX7 shRNA) lentiviral particles as previous described [13].

Determination of cell growth curve

FLO-1 and OE33 cells were infected with control or GPX7-expressing adenoviral particles or transfected with control or GPX7-expressing pcDNA plasmid (cells were under selection of 600 mg/ml G418 for 2 weeks). HET1A cells were transfected with Sc shRNA and GPX7 shRNA. Cell numbers were counted at 24h intervals using the Bio-Rad TC10 Automated Cell Counter (Bio-Rad, Hercules, California, USA) with trypan blue exclusion assay. All experiments were performed in triplicates.

Colony formation assay

FLO-1 cells were infected with 25 MOI control or GPX7-expressing adenoviral particles. 48h after infection, cells were split and seeded in the density of 500 cells/well in the 6-well plates. Cells were cultured at 37°C for another 2 weeks. Cells were then stained with 0.5% crystal violet solution. The images of the plates were analyzed using ImageJ software (NIH).

Soft agar colony formation assay

To check if GPX7 is also involved in anchorage-independent growth, soft agar colony formation assay [14] was performed. In brief, FLO-1 and OE33 cells were infected with 25 MOI control or GPX7-expressing adenoviral particles. 48h after infection, cells were split and seeded in the density of 1.0×10^5 cells/well in a 0.35% noble agar (Sigma) mixed with culture medium which was topped on a bottom agar (0.5% noble agar with medium) in the 6-well plates. Cells were cultured at 37°C for another 2 weeks. The images of the plates were captured under a microscope and were analyzed using ImageJ software (NIH).

Cell proliferation assay

To measure cell proliferation, the Click-iT EdU Assay (Life Technologies) was performed following the manufacturer's recommendation, as previously described [15]. EdU (5-ethynyl-2′-deoxyuridine) is a nucleoside analog of thymidine and is incorporated into DNA during active DNA synthesis. EdU-positive cells (20 random fields at 40X, >400 cells) were counted using ImageJ software.

Flow cytometry analysis of cell cycle progression after synchronization

To check if GPX7 expression impairs the cell cycle progression, OE33 cells were infected with Ad-CTRL and Ad-GPX7 viral particles. Cells were blocked with 2*mM* thymidine for 16h, released from the block (cultured in full medium without thymidine) for 9h and then blocked with 2 *mM* thymidine again for 16h [16]. Cells were released from the block and returned to full culture medium. Cells were harvested and fixed in 100% ethanol. Just before FACS analysis, cells were incubated with 40 μg/ml Propidium Iodide and 100 μg/ml RNase A at 37°C for 30 min and immediately subjected to FACS analysis.

Detection of cell senescence

The β-galactosidase activity was determined using a Senescence β-Galactosidase Staining Kit (Cell Signaling) following the manufacturer's protocol. In brief, OE33 and FLO-1 cells were infected with control and GPX7-expressing adenoviral particles, cells were then split into 6-well plates and cultured in serum-reduced medium (1% FBS). At 24h, 48h and 72h time points after infection, cells were fixed and incubated with β-Galactosidase Staining Solution (pH 6.0) at 37°C overnight in a dry incubator without CO_2. The next day, the plates were checked and ten ×200 fields were photographed. The β-galactosidase staining intensity was determined using ImageJ software (NIH).

Western blotting analysis

Western blot analysis was performed using standard protocols [15]. The protein concentration was determined by a Bio-Rad Protein Assay using a FLUO Star OPTIMA microplate reader (BMG). The primary antibodies were: anti-GPX7 antibody (rabbit, 1:1000, ProteinTech Group, Chicago, Illinois, USA), anti-p73 antibody (rabbit, 1:500, Bethyl, Montgomery, Texas, USA), anti-p21 antibody (mouse, 1:1000, Cell Signaling, Danvers, Massachusetts, USA), anti-p27 antibody (rabbit, 1:1000, Cell Signaling), anti-p16 antibody (rabbit, 1:1000, Cell Signaling), anti-RB antibody (mouse, 1:1000, Cell Signaling), anti-phospho-RB, ser780 (rabbit, 1:1000, Cell Signaling), anti-phospho-RB, ser807 (rabbit, 1:1000, Cell Signaling), and anti-actin antibody (rabbit, 1:1000, Cell Signaling). Horseradish peroxidase-conjugated anti-mouse (1:10,000 dilution) and anti-rabbit (1:10,000 dilution) secondary antibodies were purchased from Cell Signaling Technology.

Xenografting in nude mice

To confirm GPX7 function in vivo, OE33 cells stably expressing GPX7 or empty pcDNA vector were injected subcutaneously into 6-week-old Nu/Nu nude mice (Charles River, Wilmington, Massachusetts, USA); 2×10^6 cells per injection site (10 sites per group). Tumor masses were monitored and measured twice a week, and the tumor volume was calculated using the formula: $T_{vol} = ½ (L \times W^2)$ where T_{vol} is tumor volume, L is tumor length and W is tumor width. All mice were sacrificed when the control mice group had tumors reaching the volume of 1000 mm^3. The tumors were weighed and photographed. All animal experiments were performed in accordance with institutional guidelines and were approved by the Animal Care Review Board at the University of Vanderbilt.

Analysis of mRNA expression and DNA copy numbers of GPX7

Total RNA and DNA were isolated using the RNeasy and DNeasy mini kit (Qiagen, Valencia, California, USA). Single-stranded complementary DNA was subsequently synthesized from RNA using the iScript cDNA synthesis Kit (Bio-Rad). The sequence of GPX7 and HPRT cDNA primers was previously described [11]. The forward and reverse primers for GPX7 genomic DNA were 5′- GTGGAGGCAGGTAGAAGCTG-3′ and 5′-CAGGATCCCAGAAAAGTCCA-3′, respectively. The primers were obtained from Integrated DNA Technologies (Coralville, Iowa, USA). The quantitative real-time polymerase chain reaction (qPCR) was performed using an iCycler (Bio-Rad) with the threshold cycle number determined by the use of iCycler software version 3.0. The mRNA expression results were normalized to the average value of HPRT1 whereas the DNA copy number results were normalized to the average value of both β-Actin and GAPDH [17]. Loss of DNA copy number was considered at a relative cutoff ration of ≤0.5 whereas copy number gain was considered at cutoff ration of ≥1.3. The fold expression was calculated as previously reported [11].

DNA bisulfite treatment and pyrosequencing analysis

The DNA was bisulfite modified using an EZ DNA Methylation Gold Kit (Zymo Research, Orange, California, USA) according to the manufacturer's protocol. Five pyrosequencing assays were designed using PSQ assay design software (Qiagen) to cover a long region of GPX7 promoter from −162 to +138, relative to transcription start site (TSS) as shown in Figure 8A and Supplementary Table 1. The PCR conditions and subsequent pyrosequencing procedure were performed according to established protocols [11]. Based on control normal samples and internal quality controls provided in the software analysis, we used 10% as a cut-off value for identification of DNA hypermethylation [11].

Statistical Analysis

Data are expressed as the mean ± standard error of the mean for parametric data. Unpaired Student *t* test was performed for two independent samples. One-way analysis of variance (ANOVA) with post-test comparison was used to analyze the independent samples of 3 or more. Spearman's rank correlation analysis was used to analyze the correlation between GPX7 methylation level and gene expression. All statistical analyses were done using GraphPad Prism4 software. For all analyses, $p \leq 0.05$ is considered statistically significant.

Results

Reconstitution of GPX7 suppressed growth of OAC cells in vitro

Using stable (pcDNA-GPX7) and transient (adenoviral) reconstitution models of GPX7 in OAC cell lines (FLO-1 and OE33), we detected a significant reduction in growth rates in GPX7-expressing cells (Figure 1A–D). Concordant with these results, the reconstitution of GPX7 resulted in a significant suppression of colony formation in FLO-1 cells (Figure 1E–F). For further validation, we performed a soft agar assay using both OE33 and FLO-1 cells and found that reconstitution of GPX7 led to significantly fewer and smaller colonies ($p<0.01$) (Figure 2A–B). These data indicate that GPX7 can suppress both anchorage-dependent and -independent growth of OAC cells.

Reconstitution of GPX7 in OAC cells suppressed tumor cell proliferation and impaired cell cycle progression

Because the aforementioned data suggested a possible effect on cell proliferation, we performed the EdU assay and found that OAC cells expressing GPX7 (Ad-GPX7) have a significantly lower positive rate for EdU incorporation as compared to Ad-CTRL ($p=0.038$)

(OE33 cells are shown in Figure 3A, FLO-1 cells are shown in Supplementary Figure 1). These findings prompted us to further examine the cell cycle. We synchronized OE33 cells at the G1/S point by thymidine double block [16] followed by a release and analysis of cell cycle progression using FACS. As shown in Figure 3B, approximately half of the control cells (Ad-CTRL) had proceeded to middle S phase after 4h while only 32.4% of GPX7-expressing cells (Ad-GPX7) proceeded to early S phase, suggesting that GPX7-expressing cells had a delay in G1/S progression.

GPX7 promotes cell senescence in OAC cells in vitro

One of the key features of tumor suppressor genes is cellular senescence. Our analysis demonstrated that GPX7-expressing OAC cells (OE33 and FLO-1) had a significant increase in β-galactosidase staining ($p \leq 0.01$), as compared with control cells (Figure 4), suggesting that GPX7 can promote cell senescence in OAC cells.

GPX7 expression deregulates cell cycle and senescence components of cell signaling

As we observed growth suppression, impairment in G1/S progression, and cell senescence in GPX7-expressing OAC cells, we next examined cellular signaling components involved in these processes. Western blot analysis of FLO-1 and OE33 OAC cells that are stably expressing GPX7 (Figure 5A) or following infection with GPX7-expressing adenoviral particles (Figure 5B) demonstrated an increase in the levels of p73, p27, p21, and p16. Of note, the p16 protein was not detectable in FLO-1 cells, suggesting that it may be deleted or methylated in this cell line, a common finding in oesophageal cancers. The decrease in the phosphorylation levels of the RB protein at serine 807 and serine 780 are indicative of increased RB activity in GPX7-expressing cells. These data provide a plausible explanation consistent with the biological phenotype that we observed following reconstitution of GPX7.

Knockdown of GPX7 expression in HET1A cells promoted cellular proliferation

To confirm the tumor suppressor functions of GPX7, we knocked down GPX7 in non-malignant HET1A cells, which expresses a higher level of GPX7. As shown in Figure 6, knockdown of GPX7 resulted in significant increase in EdU rate (A) and cell growth rate (B). Western blotting analysis (C) confirmed the decrease in the levels of p73, p21, p27, and p16, and increase in the levels of phosphorylated RB in GPX7 knockdown cells (GPX7 shRNA) as compared with that in control cells.

Overexpression of GPX7 inhibited OAC tumor growth in vivo

To confirm the above results in vitro, we applied an in vivo xenografting mouse model. As shown in Figure 7, the control OE33 cells generated large tumor masses whereas the GPX7-expressing OE33 cells either failed to generate tumor mass or generated significantly smaller tumors ($p=0.004$). Of note, we performed a similar in vivo experiment using GPX3 reconstitution and failed to detect a similar tumor suppression effect (Supplementary Figure 2), suggesting that the tumor suppressor function is unique for GPX7.

Location-specific promoter DNA methylation is responsible for GPX7 downregulation in OAC

Gene mutations and allele alterations such as DNA copy number loss are involved in the downregulation of some tumor suppressor genes. However, we did not discover any missense mutation in the CDS region in cell lines originated from normal squamous epithelia (HEEC), Barrett's oesophagus (BAR-T), oesophageal adenocarcinoma (FLO-1, OE33, SKGT4, and JH-ESO-ad1), and 10 OAC samples and their matched normal oesophagus (Data available). Similarly, we did not detect DNA copy number losses of GPX7 in cell lines and OAC samples as compared with normal samples ($P>0.05$,

Supplementary Figure 3 and Table 1). These data suggested that genetic events do not play a major role in regulating GPX7 expression in OAC. We have previously shown that methylation of GPX7 could regulate its expression [11]. However, this earlier analysis was limited to a small region of the GPX7 promoter and did not take into consideration the recent observations that methylation could have location-specific effects [18–20]. Our analysis of the GPX7 promoter spanned the region from −162 to +138, relative to transcript start site (TSS) (Figure 8A and Supplementary Table 1) and demonstrated low methylation levels (<10%) in normal squamous epithelia of the oesophagus (NS) and normal glandular epithelia of the stomach (NG, Figure 8B). The Barrett's oesophagus (BO) demonstrated hypermethylation (≥10%) in all examined CpG sites except for sites from +13 to +64, suggesting that hypermethylation of GPX7 could start as early as BO. On the other hand, we found that hypermethylation of the CpG sites from +13 to +64 were unique to OAC samples ($p<0.01$) (Figure 8B–C). Of note, methylation levels of this region inversely correlated with GPX7 expression ($r=-0.37$, $p=0.001$) (Figure 8D), suggesting that location-specific methylation (+13 to +64) plays a critical role in regulating GPX7 expression. Interestingly, in cell lines CP-B, OE19, OE33 and some primary OAC (Table 1), we observed that GPX7 promoter methylation levels (≥20%) can override the observed DNA copy number gains (≥1.3 fold change) in these samples leading to downregulation of GPX7. Taken together, the results suggest that location-specific promoter hypermethylation is the major event in regulating GPX7 expression.

Discussion

GPX7 is a relatively new member of the GPX family, which has not been fully characterized. We have recently demonstrated that GPX7 can neutralize H_2O_2 and protect oesophageal epithelia from acidic bile salts-induced oxidative DNA damage through reducing intracellular reactive oxygen species (ROS) levels [10]. Because of its frequent silencing in OAC, we decided to examine its possible tumor suppressor functions. In this study, using transient and stable reconstitution of GPX7 in both in vitro and in vivo models of OAC, we have shown that GPX7 was capable of suppressing cellular proliferation and anchorage-dependent and -independent growth capacity, promote cellular senescence, and mediate a delay in G1/S progression. On the contrary, knockdown of GPX7 expression promoted cell growth and cellular proliferation in non-malignant oesophageal cells. While GPX7 promoter hypermethylation can occur at different promoter regions, our detailed analyses have demonstrated location-specific DNA promoter hypermethylation as the major event in regulating GPX7 dysfunction in OAC. Taken together, the results suggest that GPX7 possesses tumor suppressor functions that are lost through location-specific promoter methylation in OAC.

The regulation of the cell cycle is a complex cellular process where the balance between several cyclin dependent kinases and their inhibitors dictate the ultimate outcome for the cell. De-regulation of these factors leads to loss of control on cellular proliferation, a fundamental feature of tumor development [21, 22]. The loss of protein expression of p16, p21 and p27 has been shown to be one of the steps taking place during progression from BO to OAC, leading to significant impairment of cell-cycle control [23, 24]. The loss of p16 is considered to be one of the early molecular features of the development of OAC [25, 26]. p16, encoded by cyclin-dependent kinase inhibitor 2A (CDKN2A), is a classical tumor suppressor gene that plays a critical role in negatively regulating the cell cycle [27, 28]. Deletions, mutations, and promoter methylation of p16 are among the most commonly described mechanisms for silencing its expression and functions in human cancer [27]. In addition to the loss of p16 expression, inactivation of the cyclin-dependent kinase inhibitor, p27, has been shown in several tumor types, including OAC [29]. p27 plays an important role in establishing a threshold for G1 cyclin/CDK accumulation prior to activation of

CDK2 kinase and entry into the mitotic cycle [29, 30]. This finding is consistent with our results showing a delay in the G1/S progression following reconstitution of GPX7 where p27 becomes upregulated. One of the key downstream targets of p53 is p21, a protein known to play critical roles in promoting cell cycle arrest [31, 32]. p21 is a potent cyclin-dependent kinase inhibitor which regulates the cell cycle progression at G1 by binding to and inhibiting the activity of CDK2 or CDK1 complexes. We have shown that GPX7 can modulate the levels of p21 in OAC cell lines in which the p53 gene is mutant [33]. This finding indicates that GPX7 can regulate the levels of p21 in a p53-independent mechanism, and adds to the tumor suppressor capabilities of GPX7. Of note, we have shown here that one of p53 family members, p73, is upregulated upon expression of GPX7 in tumor cells. Like p53, p73 has similar tumor suppressor functions and shares many p53 target genes such as p21 [34, 35]. Therefore, the upregulation of p21 in GPX7 expressing cells was likely regulated through p73. In support of this note, our knockdown results clearly showed that loss of GPX7 expression led to the loss of expression of p73 and p21, as well as p27 and p16, accompanied by increased phospho-RB levels that rendered the cells growth advantage. We have previously shown that dysfunction of GPX7 is frequent and likely an early event occurring through BO to dysplasia stages [13]. Taken together, these results suggest that dysfunction of GPX7 may play a crucial role in Barrett's tumorigenesis through de-regulation of the key cell cycle regulators listed above.

Cellular senescence is one of mechanisms in which tumor suppressor genes exert their functions [36, 37]. We observed a significant increase in β-galactosidase staining intensity in GPX7-expressing cells as compared with control cells in both OE33 and FLO-1 cells (Figure 5). It has been known that p21 and p16, as well as RB genes are key regulators involved in both cell cycle and senescence processes [36–38]. Our Western blotting results, which showed an increase in the levels of p21 and p16 and a reduction in the levels of phospho-RB at the sites of serine 807 and serine 708 in GPX7-expressing cells as compared to controls, support the cellular senescence phenotype observed. These data demonstrate that GPX7 may execute its tumor suppressor function at least partially through promoting tumor cell senescence.

While the aforementioned results demonstrated the activation of key tumor suppressor genes upon reconstitution of GPX7 in OAC, it was essential to determine whether the biological functions can be replicated in vivo and if they are specific to GPX7 or extend to other GPx family members. Previous studies have shown that GPX3 and GPX7 were the only GPX family members that are frequently deregulated in OAC [11, 39]. Contrary to our findings showing that reconstitution of GPX7 suppressed OAC tumor growth, reconstitution of GPX3, a GPX family member that is also methylated in OAC [11, 39], failed to suppress tumor growth in vivo. These results suggest that the tumor growth suppressor functions are GPX7-specific. However, it is possible that other members of the GPx family may have similar functions as GPX7 in other cancers.

Aberrant DNA methylation is one of the most common epigenetic alterations that regulate tumor suppressor genes in cancer cells [40–42]. Recent evidences have suggested that not all CpG sites are functionally equal [18, 20]. While our earlier report analyzing a limited region of the GPX7 promoter (−38 to +11 from TSS) has suggested that methylation could regulate GPX7 [11], the extent of promoter methylation and functional relevance remained unclear. Furthermore, the possibility that genetic events could also lead to dysfunction of GPX7 were not explored. While several reports have shown that transcriptional silencing could be a result of the interaction of genetic and epigenetic events [17, 43–45], we did not detect mutations or copy number losses of GPX7 in OAC. Our comprehensive analysis of the GPX7 promoter CpG island in the present study has pointed out the region from +13 to +64 as a specific region that was associated with OAC and was significantly inversely correlated

to GPX7 expression, confirming that it is indeed a functional region of the GPX7 promoter. This finding is in line with recent literature that location-specific methylation of promoter regions plays a crucial role in regulating gene transcription in cancer [18] [19, 20]. In fact, this is further supported by our observation of downregulation of GPX7 in OAC samples with relative copy number gains where promoter hypermethylation was present (Table 1).

In conclusion, we have demonstrated that GPX7 has tumor suppressor functions through regulating key cell cycle signaling molecules. Location-specific promoter methylation mediates GPX7 silencing and the loss of its potential tumor suppressor capacity, which could be a key step in unleashing the oncogenic features driving OAC.

Supplementary Material

Refer to Web version on PubMed Central for supplementary material.

Acknowledgments

Funding Sources: This study was supported by grants from the National Institute of Health; R01CA106176, Department of Veterans Affairs, Vanderbilt SPORE in Gastrointestinal Cancer (P50 CA95103), Vanderbilt Ingram Cancer Center (P30 CA68485) and the Vanderbilt Digestive Disease Research Center (DK058404). The contents of this work are solely the responsibility of the authors and do not necessarily represent the official views of the National Cancer Institute, Department of Veterans Affairs, or Vanderbilt University.

References

1. Parkin, DM.; Pisani, P.; Ferlay, J. Global cancer statistics. Vol. 49. CA: a cancer journal for clinicians; 1999. p. 33-64.1
2. Spechler SJ, Goyal RK. Barrett's esophagus. The New England journal of medicine. 1986; 315(6): 362–371. [PubMed: 2874485]
3. Musana AK, et al. Barrett's esophagus: incidence and prevalence estimates in a rural MidWestern population. The American journal of gastroenterology. 2008; 103(3):516–524. [PubMed: 17970839]
4. Gilbert EW, et al. Barrett's Esophagus: A Review of the Literature. Journal of gastrointestinal surgery : official journal of the Society for Surgery of the Alimentary Tract. 2011; 15(5):708–718. [PubMed: 21461873]
5. Drewitz DJ, Sampliner RE, Garewal HS. The incidence of adenocarcinoma in Barrett's esophagus: a prospective study of 170 patients followed 4.8 years. The American journal of gastroenterology. 1997; 92(2):212–215. [PubMed: 9040193]
6. Shaheen NJ, Richter JE. Barrett's oesophagus. Lancet. 2009; 373(9666):850–861. [PubMed: 19269522]
7. Brigelius-Flohe R. Glutathione peroxidases and redox-regulated transcription factors. Biological chemistry. 2006; 387(10–11):1329–1335. [PubMed: 17081103]
8. Brigelius-Flohe R, Kipp A. Glutathione peroxidases in different stages of carcinogenesis. Biochimica et biophysica acta. 2009; 1790(11):1555–1568. [PubMed: 19289149]
9. Utomo A, et al. Identification of a novel putative non-selenocysteine containing phospholipid hydroperoxide glutathione peroxidase (NPGPx) essential for alleviating oxidative stress generated from polyunsaturated fatty acids in breast cancer cells. The Journal of biological chemistry. 2004; 279(42):43522–43529. [PubMed: 15294905]
10. Peng D, et al. Glutathione peroxidase 7 protects against oxidative DNA damage in oesophageal cells. Gut. 2011
11. Peng DF, et al. DNA hypermethylation regulates the expression of members of the Mu-class glutathione S-transferases and glutathione peroxidases in Barrett's adenocarcinoma. Gut. 2009; 58(1):5–15. [PubMed: 18664505]
12. Siewert JR, Feith M, Stein HJ. Biologic and clinical variations of adenocarcinoma at the esophago-gastric junction: relevance of a topographic-anatomic subclassification. J Surg Oncol. 2005; 90(3): 139–146. discussion 146. [PubMed: 15895452]

13. Peng D, et al. Glutathione peroxidase 7 protects against oxidative DNA damage in oesophageal cells. Gut. 2012; 61(9):1250–1260. [PubMed: 22157330]
14. Ochi N, et al. Protein kinase D1 promotes anchorage-independent growth, invasion, and angiogenesis by human pancreatic cancer cells. Journal of cellular physiology. 2011; 226(4):1074–1081. [PubMed: 20857418]
15. Vangamudi B, et al. t-DARPP regulates phosphatidylinositol-3-kinase-dependent cell growth in breast cancer. Molecular cancer. 2010; 9:240. [PubMed: 20836878]
16. Ma HT, Poon RY. Synchronization of HeLa cells. Methods in molecular biology. 2011; 761:151–161. [PubMed: 21755447]
17. Soutto M, et al. Epigenetic and genetic silencing of CHFR in esophageal adenocarcinomas. Cancer. 2010; 116(17):4033–4042. [PubMed: 20564104]
18. Peng D, et al. Location-specific epigenetic regulation of the metallothionein 3 gene in esophageal adenocarcinomas. PloS one. 2011; 6(7):e22009. [PubMed: 21818286]
19. Jain S, et al. Impact of the location of CpG methylation within the GSTP1 gene on its specificity as a DNA marker for hepatocellular carcinoma. PloS one. 2012; 7(4):e35789. [PubMed: 22536438]
20. van Vlodrop IJ, et al. Analysis of promoter CpG island hypermethylation in cancer: location, location, location! Clinical cancer research : an official journal of the American Association for Cancer Research. 2011; 17(13):4225–4231. [PubMed: 21558408]
21. Sandhu C, Slingerland J. Deregulation of the cell cycle in cancer. Cancer detection and prevention. 2000; 24(2):107–118. [PubMed: 10917130]
22. Vermeulen K, Van Bockstaele DR, Berneman ZN. The cell cycle: a review of regulation, deregulation and therapeutic targets in cancer. Cell proliferation. 2003; 36(3):131–149. [PubMed: 12814430]
23. Merola E, et al. Immunohistochemical evaluation of pRb2/p130, VEGF, EZH2, p53, p16, p21waf-1, p27, and PCNA in Barrett's esophagus. Journal of cellular physiology. 2006; 207(2): 512–519. [PubMed: 16447267]
24. Spechler SJ. Barrett's esophagus: a molecular perspective. Current gastroenterology reports. 2005; 7(3):177–181. [PubMed: 15913475]
25. Bian YS, et al. p16 inactivation by methylation of the CDKN2A promoter occurs early during neoplastic progression in Barrett's esophagus. Gastroenterology. 2002; 122(4):1113–1121. [PubMed: 11910361]
26. Wong DJ, et al. p16(INK4a) lesions are common, early abnormalities that undergo clonal expansion in Barrett's metaplastic epithelium. Cancer Res. 2001; 61(22):8284–8289. [PubMed: 11719461]
27. Liggett WH Jr. Sidransky D. Role of the p16 tumor suppressor gene in cancer. Journal of clinical oncology : official journal of the American Society of Clinical Oncology. 1998; 16(3):1197–1206. [PubMed: 9508208]
28. Roussel MF. The INK4 family of cell cycle inhibitors in cancer. Oncogene. 1999; 18(38):5311–5317. [PubMed: 10498883]
29. Lee J, Kim SS. The function of p27 KIP1 during tumor development. Experimental & molecular medicine. 2009; 41(11):765–771. [PubMed: 19887899]
30. Sicinski P, Zacharek S, Kim C. Duality of p27Kip1 function in tumorigenesis. Genes & development. 2007; 21(14):1703–1706. [PubMed: 17639075]
31. Abukhdeir AM, Park BH. P21 and p27: roles in carcinogenesis and drug resistance. Expert reviews in molecular medicine. 2008; 10:e19. [PubMed: 18590585]
32. McChesney PA, et al. Cofactor of BRCA1: a novel transcription factor regulator in upper gastrointestinal adenocarcinomas. Cancer Res. 2006; 66(3):1346–1353. [PubMed: 16452188]
33. Boonstra JJ, et al. Verification and unmasking of widely used human esophageal adenocarcinoma cell lines. Journal of the National Cancer Institute. 2010; 102(4):271–274. [PubMed: 20075370]
34. Zawacka-Pankau J, et al. p73 tumor suppressor protein: a close relative of p53 not only in structure but also in anti-cancer approach? Cell Cycle. 2010; 9(4):720–728. [PubMed: 20160513]
35. Flores ER, et al. Tumor predisposition in mice mutant for p63 and p73: evidence for broader tumor suppressor functions for the p53 family. Cancer cell. 2005; 7(4):363–373. [PubMed: 15837625]

36. Shay JW, Roninson IB. Hallmarks of senescence in carcinogenesis and cancer therapy. Oncogene. 2004; 23(16):2919–2933. [PubMed: 15077154]

37. Collado M, Blasco MA, Serrano M. Cellular senescence in cancer and aging. Cell. 2007; 130(2): 223–233. [PubMed: 17662938]

38. Rayess H, Wang MB, Srivatsan ES. Cellular senescence and tumor suppressor gene p16. International journal of cancer. Journal international du cancer. 2012; 130(8):1715–1725. [PubMed: 22025288]

39. Lee OJ, et al. Hypermethylation and loss of expression of glutathione peroxidase-3 in Barrett's tumorigenesis. Neoplasia. 2005; 7(9):854–861. [PubMed: 16229808]

40. Esteller M, et al. Cancer epigenetics and methylation. Science. 2002; 297(5588):1807–1808. discussion 1807-8. [PubMed: 12229925]

41. Jones PA. DNA methylation and cancer. Oncogene. 2002; 21(35):5358–5360. [PubMed: 12154398]

42. Herman JG, Baylin SB. Gene silencing in cancer in association with promoter hypermethylation. The New England journal of medicine. 2003; 349(21):2042–2054. [PubMed: 14627790]

43. Tamura G. Alterations of tumor suppressor and tumor-related genes in the development and progression of gastric cancer. World journal of gastroenterology : WJG. 2006; 12(2):192–198. [PubMed: 16482617]

44. Jarrard DF, et al. Deletional, mutational, and methylation analyses of CDKN2 (p16/MTS1) in primary and metastatic prostate cancer. Genes, chromosomes & cancer. 1997; 19(2):90–96. [PubMed: 9171999]

45. Knudson AG. Two genetic hits (more or less) to cancer. Nature reviews. Cancer. 2001; 1(2):157–162.

What is already known about this subject?

- Glutathione peroxidase-7 (GPX7) is a recently identified member of the GPx family.
- Earlier studies have shown that GPX7 is frequently downregulated in oesophageal adenocarcinomas (OACs).
- GPX7 protects oesophageal epithelial cells against acidic bile salts-induced oxidative DNA damage, double-strand breaks and cell death through reduction of intracellular ROS level.
- Loss of GPX7 promotes accumulation of intracellular ROS and oxidative DNA damage.

What are the new findings?

- This study demonstrates that GPX7 can regulate the cellular growth pattern and the levels of p27, p21 and p16 and phospho-RB proteins; key cell cycle regulators.
- In addition, GPX7 regulates the levels of p73, an important family member of the tumor suppressor p53.
- Reconstitution of GPX7 expression in OAC cells suppresses their tumor growth capacity in xenograft mouse model.
- GPX7 dysfunction in OAC is predominantly regulated by promoter DNA hypermethylation, in particular the CpG sites from +13 to +64, rather than the genetic mutation and copy number loss.

How might it impact on clinical practice in the foreseeable future?

- This study provides direct evidence of the role GPX7 plays in oesophageal tumorigenesis highlighting previously unknown novel tumor suppressor functions of GPX7.
- Taken together with our previous studies, GPX7 is a dual function protein that has potent antioxidant and tumor suppressor functions that could play an important role in protecting the genomic integrity of esophageal cells. Therefore, it is possible that patients with loss of GPX7 could be at higher risk of progression towards oesophageal adenocarcinoma.

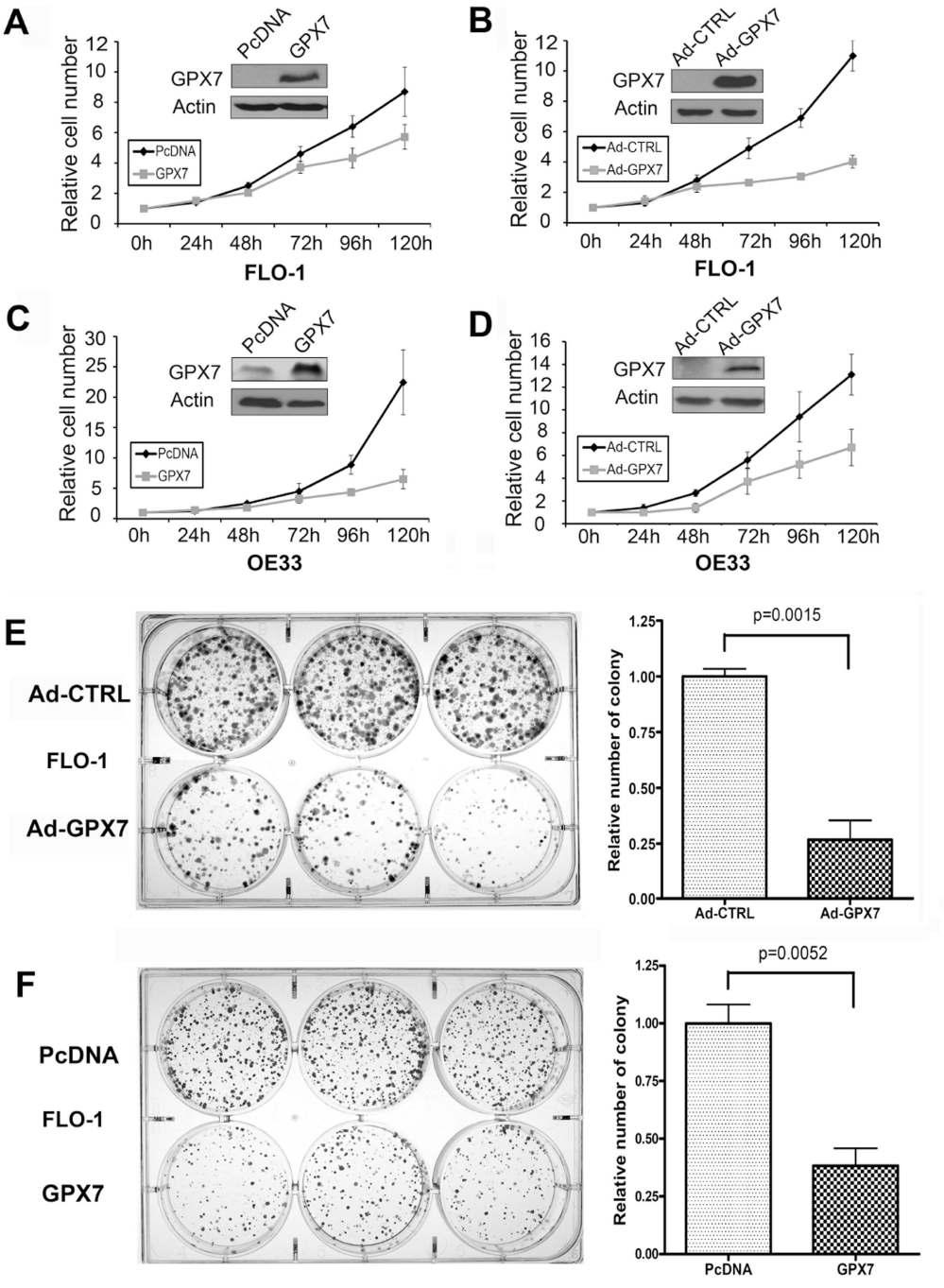

Figure 1. Reconstitution of GPX7 expression suppresses OAC cell growth in vitro

A–D) Growth curves were graphed based on cell counting using trypan blue assay after reconstitution of expression of GPX7 in FLO-1 (A–B) and OE33 (C–D) OAC cell lines. Both pcDNA stable (A and C) and transient adenoviral (Ad) (B and D) reconstitution of GPX7 demonstrate significant reduction in cell growth, as compared to controls ($p<0.01$ at 96h and 120h points). Western blots are included to demonstrate the levels of GPX7. **E–F)** Colony formation assay in 500 OAC cells (FLO-1) using adenoviral (Ad) (E) or pcDNA stable (pcDNA) (F) reconstitution of GPX7 demonstrate significant reduction in the number and size of colonies ($p<0.01$). Quantification is shown on the right panels.

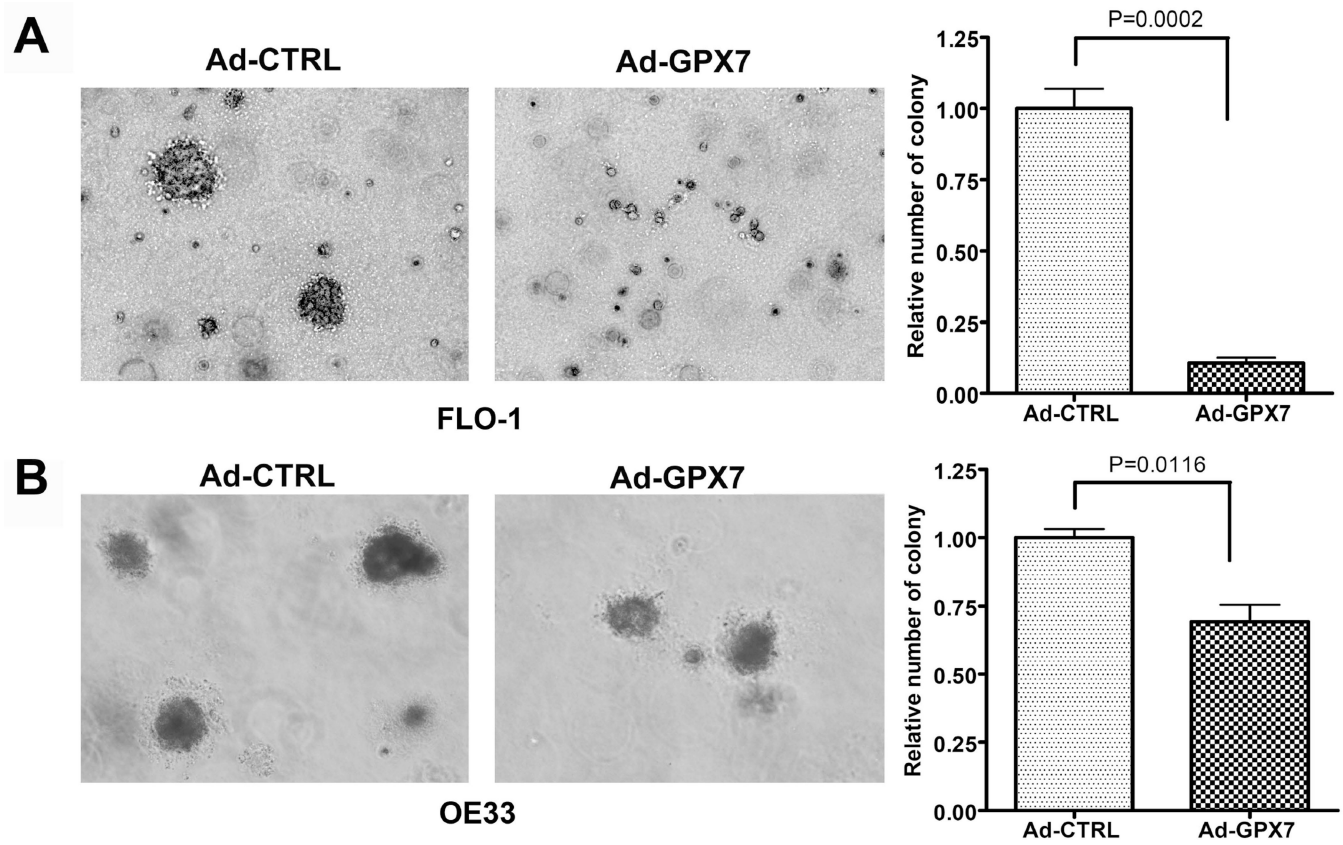

Figure 2. GPX7 suppresses anchorage-independent growth

A–B) Soft agar colony formation assay in FLO-1 cells (A) and OE33 cells (B). In both **A** and **B**, cells with GPX7-expressing adenoviral particles (Ad-GPX7) formed significantly smaller and fewer colonies, as compared to control (Ad-CTRL) ($p<0.01$). Quantification of the data is shown on the right panels.

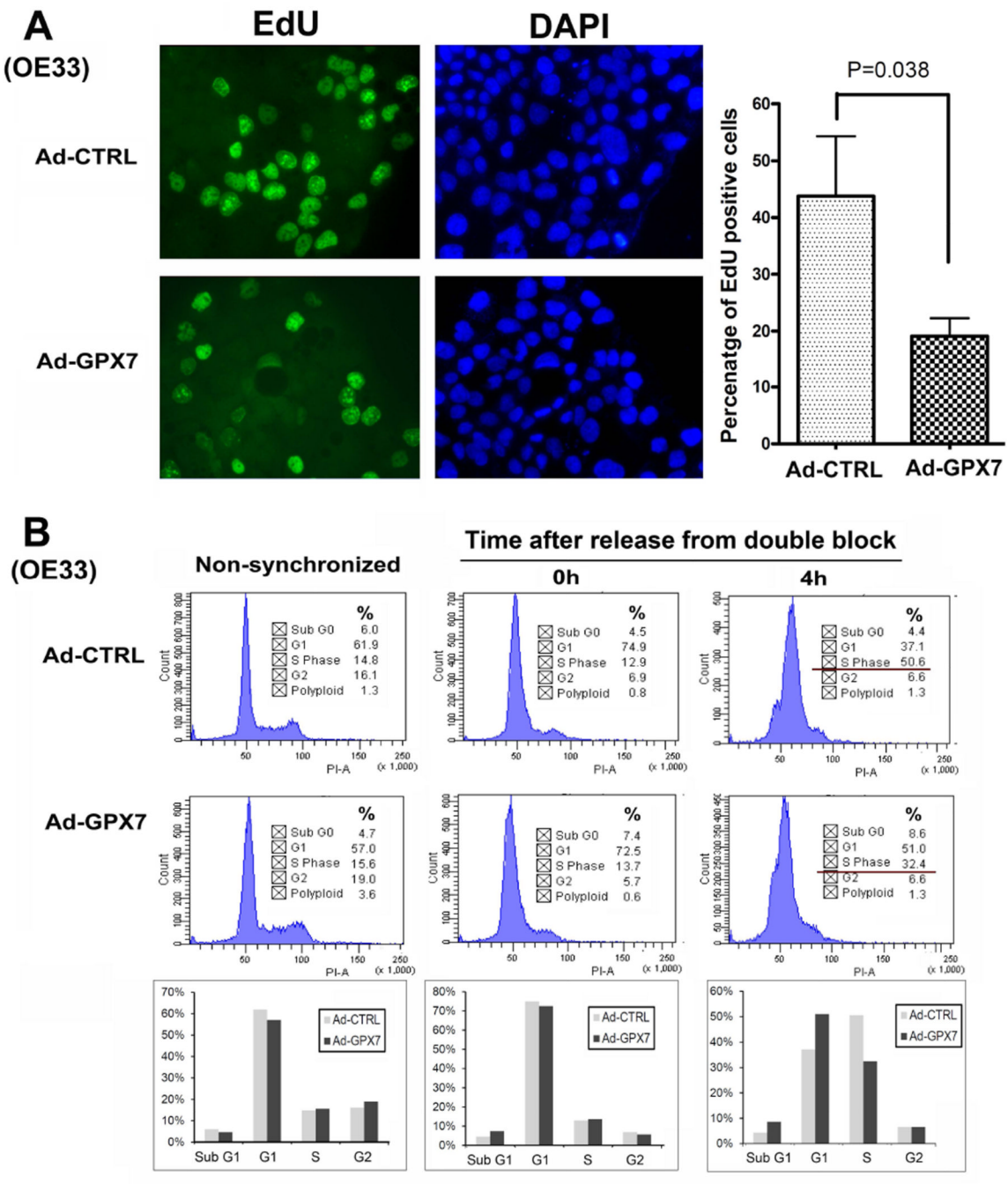

Figure 3. GPX7 expression inhibits tumor cell proliferation and delays the G1/S progression

A) EdU fluorescence staining (green) demonstrates a significant decrease of nuclear incorporation of EdU in OE33 cells following the expression of GPX7 (Ad-GPX7), as compared to control cells (Ad-CTRL) (p=0.038). The right panel displays the quantitative data. **B)** Flow cytometry analysis of cell cycle progression of OE33 cells after double thymidine block and release for 4h; results demonstrate that approximately half of the control cells (Ad-CTRL) had proceeded to middle S phase after 4h while only 32.4% of GPX7-expressing cells (Ad-GPX7) proceeded to the early S phase. Representative flow cytometry histograms and quantification graphs are shown.

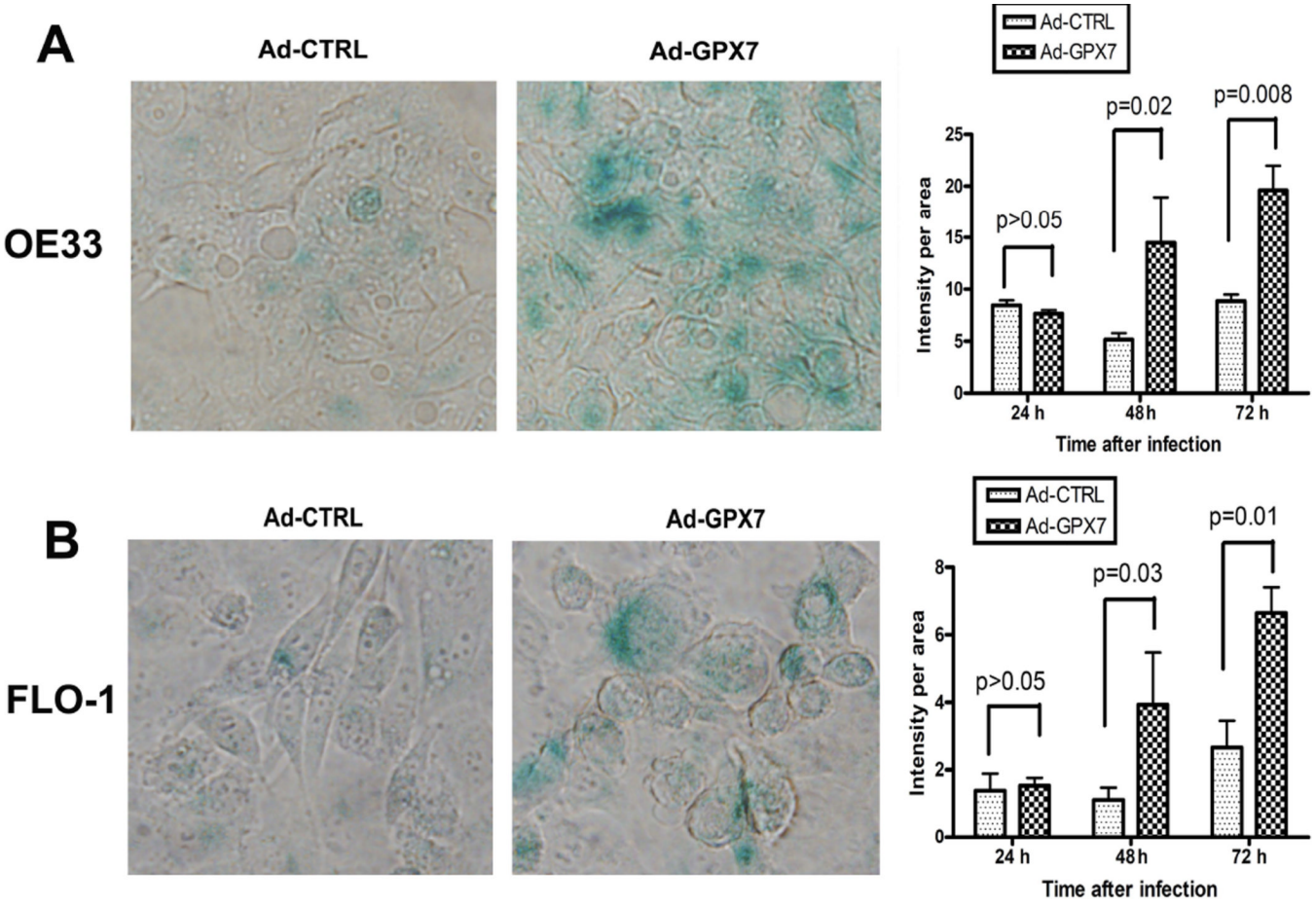

Figure 4. GPX7 promotes cell senescence in OAC cells in vitro

A–B) Representative images of β-galactosidase staining of GPX7-expressing (Ad-GPX7) and control (Ad-CTRL) OE33 (A) and FLO1 (B) cells at 72h following serum deprivation (1% FBS) ($p \leq 0.01$). The right panels display quantitative results of the β-galactosidase staining intensity at 24h, 48h and 72h time points of serum deprivation (1% FBS).

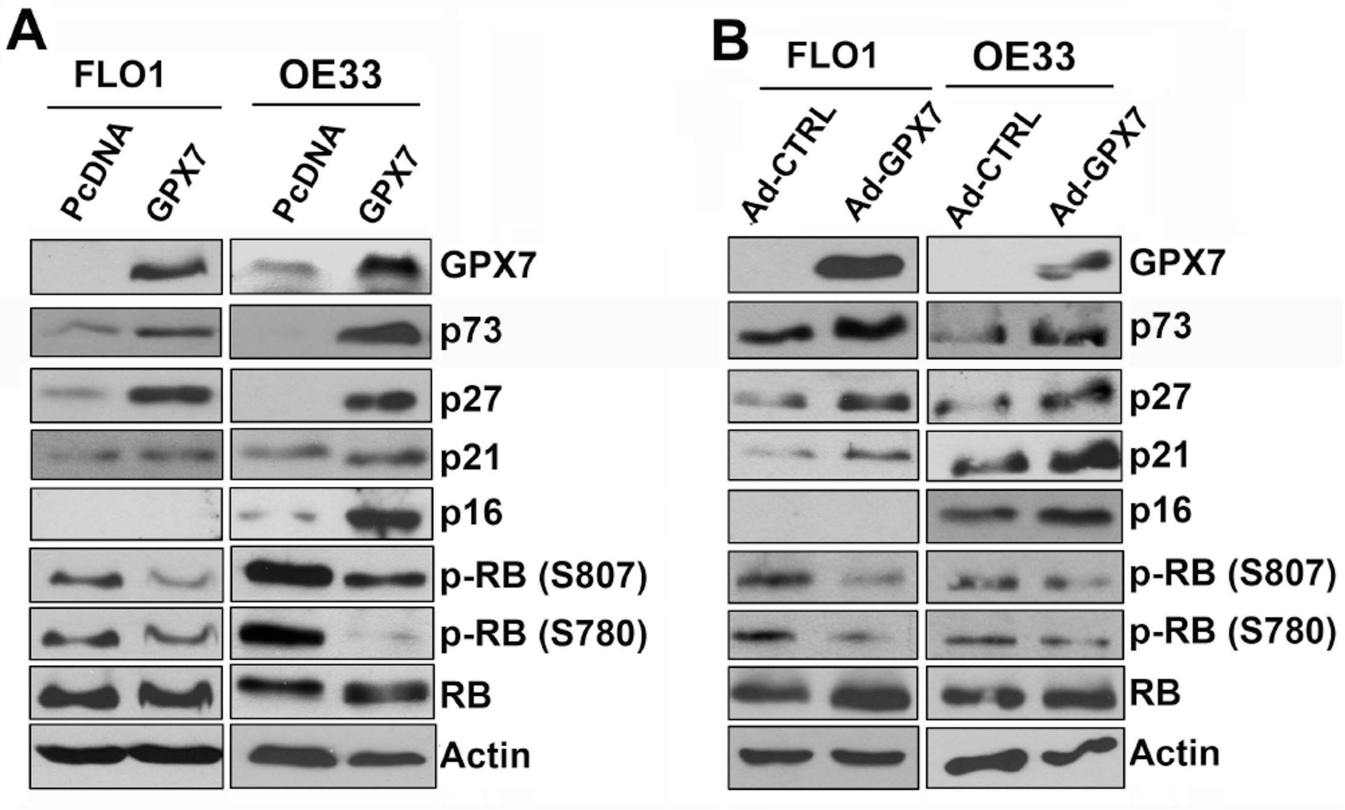

Figure 5. GPX7 regulates the protein levels of tumor suppressor genes

A–B) Western blot analysis is shown for FLO-1 and OE33 OAC cells that are stably expressing GPX7 (5A) or following infection with GPX7-expressing adenoviral particles (5B). An increase in the levels of p73, p27, p21, and p16 and a decrease in phosphorylated RB (p-RB) were detected (FLO-1 cell line is silent for p16).

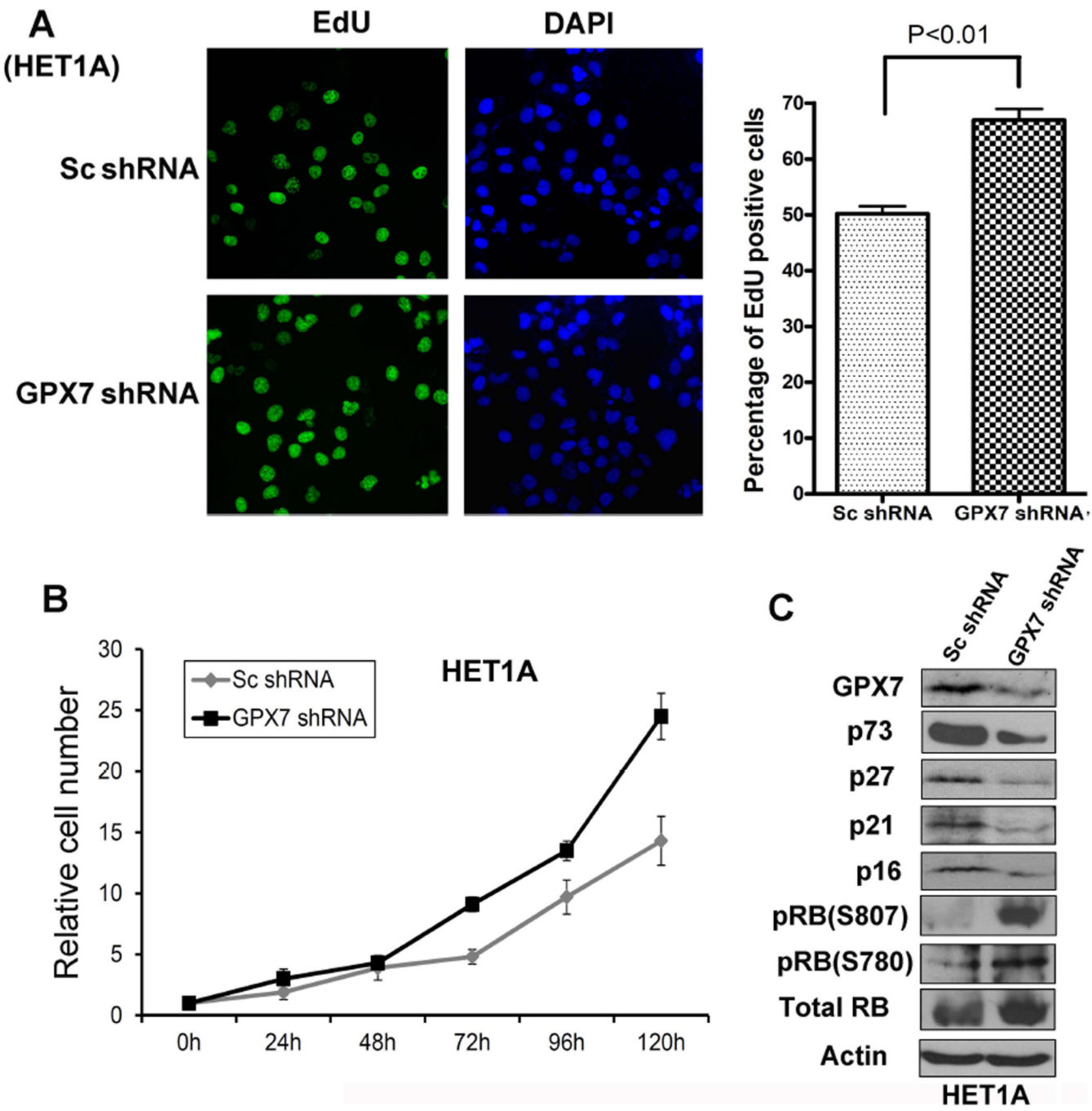

Figure 6. Knockdown of GPX7 expression renders cell growth advantage

HET1A (an immortalized normal esophageal cell line) cells were stably transfected with GPX7 specific shRNA (GPX7 shRNA) and control scramble shRNA (Sc shRNA). **A)** EdU cell proliferation assay displays that knockdown of GPX7 expression (GPX7 shRNA) led to a significant increase in EdU positive rate, indicating a higher cellular proliferation rate. The left panel shows the representative EdU and DAPI images and the right panel shows the quantification using ImageJ software. **B)** Growth curve shows faster growth rate of GPX7-knockdown cells as compare to control cells ($p<0.05$ at 72h, 96h and 120h time points). **C)**

Western blotting analysis demonstrates a reduction in the levels of p73, p27, p21, and p16 proteins and an increase of phospho-RB following GPX7 knockdown in HET1A cells.

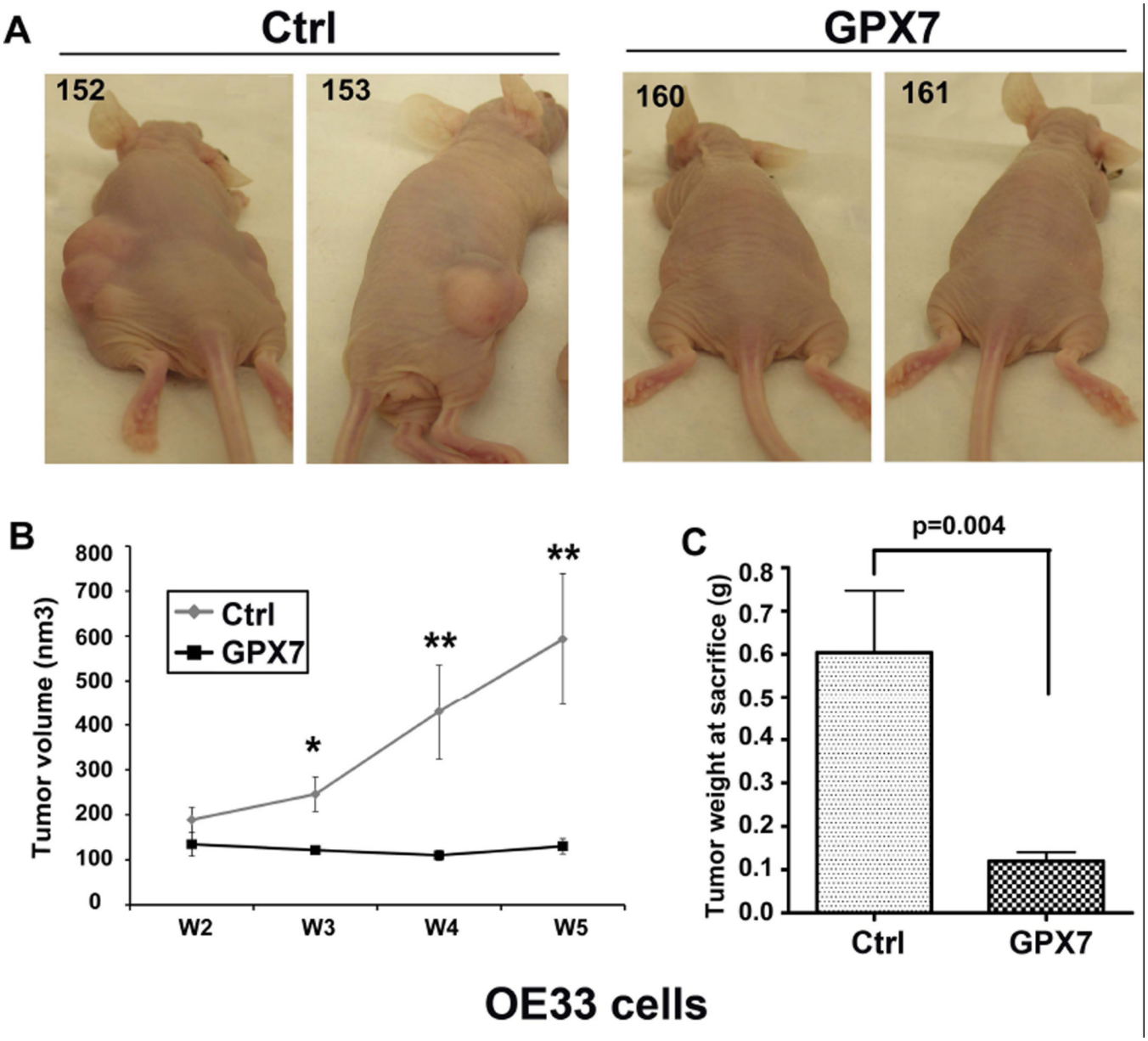

Figure 7. Reconstitution of GPX7 expression in OAC cells suppresses tumor growth in vivo

A) OE33 cells stably expressing GPX7 or empty pcDNA vector (control) were subcutaneously xenografted into Nu/Nu nude mice. Representative images are shown. **B)** Tumor volume was monitored and graphed as shown (*, $p<0.05$; **, $p<0.01$). **C)** A comparison of the weight of resected tumors is shown. GPX7-expressing tumors were significantly smaller than controls ($p=0.004$).

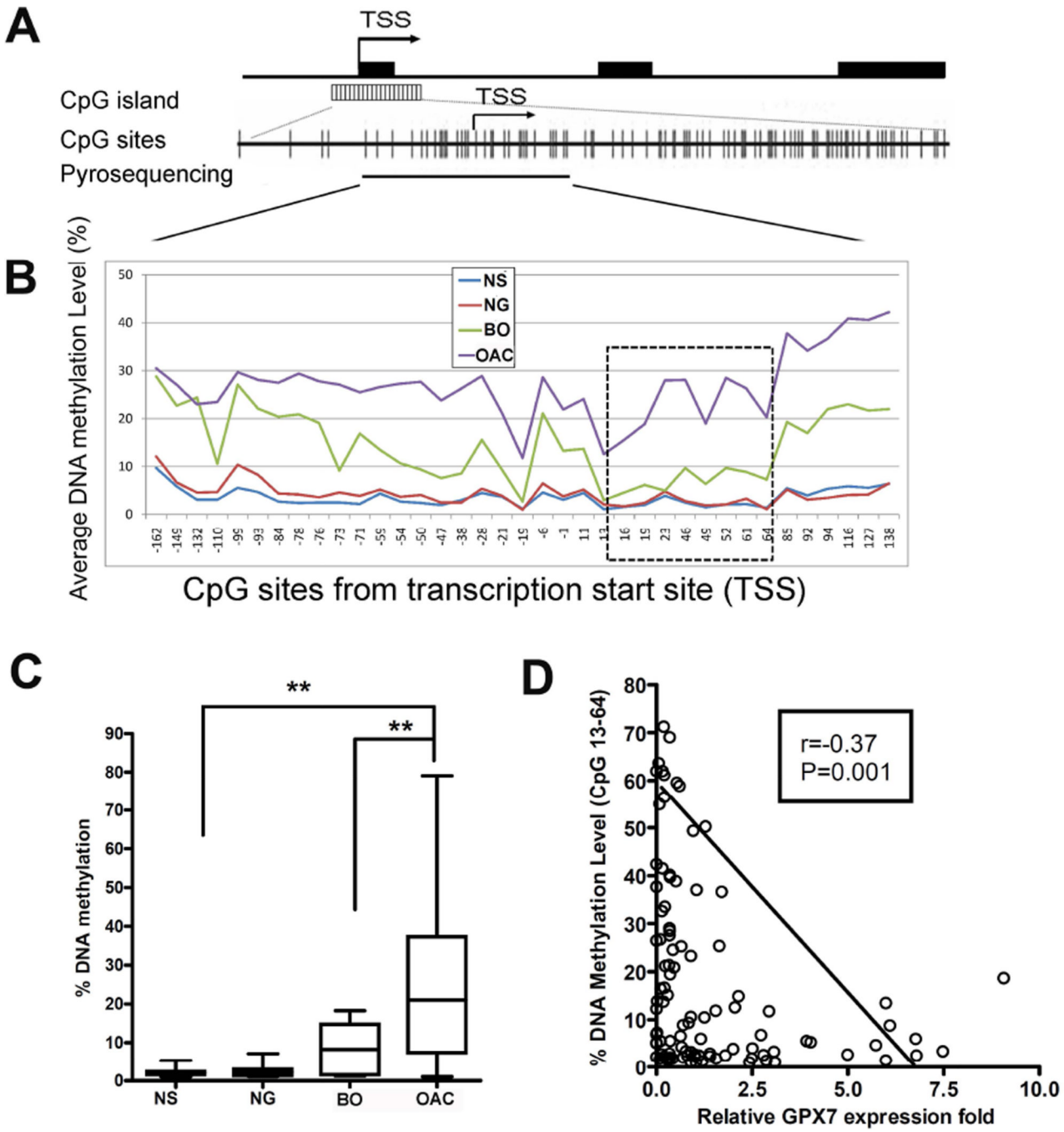

Figure 8. Location-specific DNA methylation of GPX7 promoter regulates GPX7 expression

A) A schematic chart shows GPX7 genomic structure. GPX7 has 3 exons as shown in black boxes. A CpG island with dense CpG sites is present around the transcription start site (TSS); each vertical bar represents one CpG site. Pyrosequencing assays that covered CpG sites from −162 to +138, relative to TSS were designed (Supplementary Table 1). **B)** Summary of pyrosequencing results in normal oesophageal squamous epithelia (NS), normal gastric mucosa (NG), Barrett's oesophagus (BO) and oesophageal adenocarcinoma (OAC) (additional details in Table 1). Hypermethylation of CpG sites from +13 to +64 (dash-line square) was only seen in OAC. **C)** Comparison of the average DNA methylation levels

(CpG sites from +13 to +64) in NS, NG, BO, and OAC samples. **D)** Spearman correlation analysis demonstrated inverse correlation between methylation levels (+13 to +64) and GPX7 mRNA expression fold ($r=-0.37$, $p=0.001$).

Table 1

GPX7 DNA copy number, methylation level, and mRNA expression in oesophageal cell lines and primary tumors

	Sample	Relative Fold DNA Copy Number†	DNA Methylation Level (%)‡	Relative Fold mRNA Expression¶
Normal#	N1–15	1.0	2.3	1.1
Normal	HEEC	1.0	3	2.1
Oeso	EPC2	0.8	20	1.2
Cell lines	HET1A	0.8	16	0.8
	BAR-T	1.0	47	0.4
	BAR-T10	1.2	47	0
	CP-A	0.7	20	0.1
	CP-B	1.5	53	0
OAC cell lines	SKGT4	1.1	88	0
	OE33	1.6	22	0.6
	OE19	2.1	77	0
	JH-ESO-ad1	1.0	30	0.1
	FLO-1	0.7	80	0
	1 T	1.1	14	0.2
	10 T	1.3	57	0.2
	11 T	1.5	49	1.0
	12 T	0.5	40	0.3
	13 T	1.4	13	2.1
	14 T	3.1	71	0.2
	15 T	1.7	14	1.7
	16 T	1.9	37	0.0
	17 T	1.2	5	5.7
	18 T	1.3	25	0.4
	19 T	1.9	1	2.4
	2 T	0.8	36	0.4
Primary OAC	**20 T**	1.3	61	0.2
	22 T	1.0	50	1.3
	23 T	1.5	35	0.3
	24 T	0.9	40	0.4
	25 T	0.8	17	0.6
	26 T	1.0	12	1.6
	27 T	0.6	21	0.8
	29 T	0.8	8	1.2
	3 T	1.1	9	0.8
	30 T	0.9	3	1.4
	31 T	0.6	2	2.5
	32 T	0.8	14	5.0
	33 T	0.8	33	0.2

Sample	Relative Fold DNA Copy Number†	DNA Methylation Level (%)‡	Relative Fold mRNA Expression¶
34 T	1.5	2	6.0
35 T	1.2	19	1.9
4 T	1.2	15	2.1
5 T	1.3	34	0.2
6 T	2.9	69	0.4
7 T	2.6	21	0.3
8 T	2.1	42	0.2
9 T	1.0	33	0.1

†DNA copy number was determined using qPCR, normalized to both GAPDH and Actin and compared to average of 15 normal oesophageal epithelial samples. The relative fold of GPX7 copy number in diploid normal samples is 1.0.

‡The average DNA methylation levels (%) of the CpG sites from +16 to +64 (relative to TSS) are shown.

¶The relative fold mRNA expression of GPX7 was determined by qRT-PCR, normalized to HPRT and compared to average of normal oesophageal epithelial samples.

#The average values of 15 normal oesophageal epithelial samples are shown. Samples with DNA copy number gains are shown in bold. Grey shaded rows demonstrate samples with copy number gains where DNA hypermethylation (≥ 20%) led to downregulation of GPX7 mRNA expression.